Paleoceanography and Paleoclimatology

RESEARCH ARTICLE
10.1029/2020PA004016

Complex Interactions Between Large Igneous Province Emplacement and Global-Temperature Changes During the Cenomanian-Turonian Oceanic Anoxic Event (OAE 2)

L. M. E. Percival[1], N. A. G. M. van Helmond[2], D. Selby[3,4], S. Goderis[1], and P. Claeys[1]

[1]Analytical, Environmental and Geochemistry Group, Brussels, Belgium, [2]Department of Earth Sciences, Utrecht University, Utrecht, The Netherlands, [3]Department of Earth Sciences, Durham University, Durham, UK, [4]State Key Laboratory of Geological Processes and Mineral Resources, School of Earth Resources, China University of Geosciences, Wuhan, China

Key Points:
- Osmium-isotope records of volcanism during OAE 2 are directly compared to paleotemperature records from the same sites for the first time
- Plenus Cold Event cooling is confirmed to have been diachronous and likely caused by enhanced CO_2 drawdown rather than reduced volcanism
- High global temperatures were maintained during OAE 2 long after LIP activity declined, likely aided by reduced silicate weathering rates

Supporting Information:
- Supporting Information S1

Correspondence to:
L. M. E. Percival,
lawrence.percival@vub.be

Citation:
Percival, L. M. E., van Helmond N. A. G. M., Selby, D., Goderis, S., & Claeys, P. (2020). Complex interactions between large igneous province emplacement and global-temperature changes during the Cenomanian-Turonian oceanic anoxic event (OAE 2). *Paleoceanography and Paleoclimatology*, *35*, e2020PA004016. https://doi.org/10.1029/2020PA004016

Received 19 JUN 2020
Accepted 17 SEP 2020
Accepted article online 26 SEP 2020

Abstract Super greenhouse temperatures at the onset of the Cenomanian-Turonian oceanic anoxic event (OAE 2) have been widely linked with large igneous province (LIP) volcanic activity. However, the extent to which volcanism influenced subsequent climate changes throughout OAE 2, such as global cooling during the Plenus Cold Event (PCE) early in the OAE, and the subsequent return to very warm conditions through the second part of the crisis remain less clear. Here, new osmium-isotope ($^{187}Os/^{188}Os$) data are presented from the northeastern margin of the proto-North Atlantic Ocean (ODP Leg 174AX Bass River, NJ, USA). The results are consistent with previously published OAE 2 records and are similarly interpreted as documenting LIP activity while further demonstrating the ability to use osmium-isotope stratigraphy as a global chemostratigraphic marker in open-ocean records. Correlations of $^{187}Os/^{188}Os$ and sea-surface temperature trends at Bass River and other sites show that the earliest PCE cooling coincided with intense volcanism, but that LIP activity began to decline during or soon after the cold pulse. These temporal relationships support previous hypotheses that the PCE was regionally diachronous and likely caused by enhanced carbon sequestration via organic-matter burial and silicate weathering, rather than a period of volcanic quiescence, while the persistently warm conditions later in OAE 2 were linked to reduced silicate weathering rather than sustained volcanism. These findings highlight the complex interactions between LIP emplacement and climate responses during OAE 2, reemphasizing the need for similar correlations between volcanism and paleotemperature proxy data for other major events in Earth's history.

1. Introduction

The mid-Cretaceous Cenomanian-Turonian oceanic anoxic event (OAE 2: ~94 Ma) represented one of the most severe environmental perturbations of the Mesozoic Era and was characterized by the development of oxygen-depleted water columns throughout much of the global ocean (see review by Jenkyns, 2010). The widespread anoxic/euxinic conditions greatly promoted the burial of organic matter in seafloor sediments, resulting in the depletion of isotopically light carbon (^{12}C) in seawater. This phenomenon is expressed in sedimentary records of the Cenomanian-Turonian boundary (CTB) by a globally documented positive carbon-isotope excursion (CIE) of up to 7‰ (Vienna Peedee belemnite) in carbonate material and both bulk and compound-specific organic matter, which is currently used to define the base of the OAE 2 stratigraphic level (e.g., Arthur et al., 1988; Jarvis et al., 2011; Owens et al., 2018; Tsikos et al., 2004; van Bentum et al., 2012). Several CTB archives further illustrate this enhanced drawdown of biotic carbon through the preservation of meter-thick, millimeter-laminated, organic-rich shales that record the positive CIE and mark the OAE 2 level lithologically (e.g., Arthur & Premoli-Silva, 1982; Dickson et al., 2017; Jarvis et al., 2011; Schlanger & Jenkyns, 1976; Tsikos et al., 2004). In addition to widespread anoxia/euxinia, the OAE was marked by numerous other environmental perturbations. Most notably, a sea-surface temperature (SST) rise during OAE 2 has been documented from records in both hemispheres and spanning multiple ocean basins, likely occurring as an abrupt warming around the onset of the OAE following an increase in atmospheric pCO_2 (e.g., Barclay et al., 2010; Forster et al., 2007; Robinson et al., 2019; Sinninghe Damsté et al., 2010; Voigt et al., 2006). These warm conditions and high pCO_2 levels were largely sustained

throughout the remainder of OAE 2 and into the earliest Turonian times that followed (Forster et al., 2007; Jarvis et al., 2011; O'Brien et al., 2017; Robinson et al., 2019; van Helmond et al., 2014, 2015), apart from a transient spell of climate cooling during the early part of the OAE, called the Plenus Cold Event (PCE).

The PCE is named for the belemnite species *Praeactinocamax plenus*, which was one of many boreal fauna that spread southward into Europe, the Western Interior Seaway, and northern parts of the Tethys and proto-North Atlantic oceans at that time (e.g., Gale & Christensen, 1996; Jefferies, 1962, 1963; Kuhnt et al., 1986; van Helmond et al., 2016). A shift to colder climates is also evidenced by SST drops that have been documented in several stratigraphic archives of OAE 2 and is generally considered to reflect a temporary reduction in atmospheric pCO_2 levels during the PCE (e.g., Barclay et al., 2010; Forster et al., 2007; Jarvis et al., 2011; Paul et al., 1999; Sinninghe Damsté et al., 2010; van Helmond et al., 2014, 2015). However, the exact timing of the cooling has been proposed as being diachronous across individual geographic regions as a result of local processes and/or ocean-circulation patterns (O'Connor et al., 2020). The shift to cold conditions apparently stimulated localized water-column reoxygenation (Clarkson et al., 2018; Friedrich et al., 2006; Jenkyns et al., 2017; Leckie et al., 1998; van Bentum et al., 2009), leading to a reduction in organic-matter burial, at least in some settings. This decrease in organic-carbon burial during the PCE is clearly shown at several sites by a reduction in organic-carbon content and/or a decline in $\delta^{13}C$ values back toward pre-OAE 2 ratios in strata broadly correlative with evidence for the climate cooling (e.g., Eastbourne, Anglo-Paris Basin, UK, and Pont d'Issole, Vocontian Basin, SE France; Jarvis et al., 2011; O'Connor et al., 2020; see also overview by Tsikos et al., 2004).

This study evaluates the possible links between global temperature changes during OAE 2 and the emplacement of one or more large igneous provinces (LIPs) during the latest Cenomanian. Representing the formation of millions of cubic kilometers of magmatic material (chiefly tholeiitic basalts) into/onto the Earth's crust within a geologically short space of time (Bryan & Ferrari, 2013; Kerr, 2014), LIPs have been linked to several Phanerozoic environmental crises/extinction events (see reviews by Bond & Wignall, 2014; Courtillot & Renne, 2003). Radioisotopic dating of basalts from the Caribbean-Colombian Plateau and High Arctic LIP suggests that at least some of the volcanic activity on those provinces was broadly coeval with the Cenomanian-Turonian transition (e.g., Kingsbury et al., 2018; Snow et al., 2005; Tegner et al., 2011), with eruptions possibly also occurring on the Greater Ontong-Java Plateau and Madagascan Province around that time (Kuroda et al., 2007; Neal et al., 1997; Storey et al., 1995). However, the relative inaccessibility of preserved material from those LIPs for precise dating means that the main evidence of LIP emplacement immediately prior to and during OAE 2 comes from a range of geochemical proxies of volcanism that show excursions in uppermost Cenomanian strata (e.g., Holmden et al., 2016; Jones & Jenkyns, 2001; Kuroda et al., 2007; Scaife et al., 2017; Snow et al., 2005; Sweere et al., 2018). In recent years, sedimentary records of seawater osmium (Os) isotope compositions (specifically $^{187}Os/^{188}Os$) have been increasingly utilized as the most reliable of these geochemical markers for Cenomanian-Turonian records (Du Vivier et al., 2014; Du Vivier, Selby, et al., 2015; Jones et al., 2020; Schröder-Adams et al., 2019; Sullivan et al., 2020; Turgeon & Creaser, 2008).

1.1. Os Isotopes as a Marker of LIP Emplacement Prior to and During OAE 2

Past seawater Os-isotope compositions ($^{187}Os/^{188}Os_{(i)}$) are calculated from the modern-day $^{187}Os/^{188}Os$ ratio measured in a sedimentary rock by accounting for the amount of postdepositional decay of rhenium (specifically ^{187}Re) to ^{187}Os, assuming that the age of the sample is known and that the sedimentary system remained closed with respect to the two elements throughout its burial history (Cohen et al., 1999). Primitive Os derived from the mantle or meteorite material has $^{187}Os/^{188}Os \sim 0.13$ (Allègre et al., 1999; Meisel et al., 2001), whereas riverine Os sourced from weathering of the continental crust is typically much more radiogenic (modern-day average riverine $^{187}Os/^{188}Os \sim 1.4$; Peucker-Ehrenbrink & Jahn, 2001). For all studied stratigraphic archives of OAE 2, spanning multiple ocean basins around the world, there is a clear shift in recorded $^{187}Os/^{188}Os_{(i)}$ values from approximately 0.6–1 down to ~0.2 just below the base of the OAE level sensu stricto as defined by the positive CIE, indicating an increased flux of mantle-derived Os from LIP activity to the global ocean relative to riverine runoff of the element from weathering of the continental crust and the comparatively consistent mid-ocean ridge and cosmogenic inputs (Du Vivier et al., 2014; Du Vivier, Selby, et al., 2015; Jones et al., 2020; Schröder-Adams et al., 2019; Sullivan et al., 2020; Turgeon & Creaser, 2008). A global-scale documentation of this shift is consistent

with the seawater-residence time of Os (on the order of tens of kiloyears; Peucker-Ehrenbrink & Ravizza, 2000; Rooney et al., 2016), longer than the mixing time of the ocean (~1 kyr today). Thus, the $^{187}Os/^{188}Os$ seawater composition is generally homogenous throughout the global ocean while still responding to geologically rapid changes in the sources to that inventory, except in hydrographically restricted basins with a very low basin-ocean water-mass exchange, where the Os-isotope composition might be dominated by local inputs (e.g., Dickson et al., 2015; Du Vivier et al., 2014; Paquay & Ravizza, 2012; Rooney et al., 2016).

Strata recording an unradiogenic seawater Os-isotope composition persist throughout the lower part of the OAE 2 level and typically also feature a relatively high concentration of "common" ^{192}Os (the best representation of the sedimentary Os content at the time of deposition). The elevated ^{192}Os contents are typically manifested as distinct peaks, which have been interpreted as reflecting multiple pulses in LIP volcanism (see Jones et al., 2020; Sullivan et al., 2020; Turgeon & Creaser, 2008). Os released from nonvolcanic basalt-seawater interactions might have acted as an additional source of the element to the ocean and contributed toward the documented peaks in sedimentary ^{192}Os content, but the relatively low Os concentration of basaltic rocks compared to submarine volcanic emissions suggests that such interactions were unlikely to have been the sole cause of the ^{192}Os spikes or shift to unradiogenic isotopic compositions (see Du Vivier et al., 2014). Recently, the PCE was proposed as having occurred during a spell of volcanic quiescence between two pulses of LIP volcanism evidenced from stratigraphic ^{192}Os peaks recorded in the Iona #1 core (Maverick Basin, TX, USA), with the resultant decrease in CO_2 emissions causing the climate cooling (Sullivan et al., 2020). However, an alternative model stipulates that there was a pulse (or at least a continuation) of intense volcanic activity throughout the time of the PCE (see Jenkyns et al., 2017; Zheng et al., 2013), in which case the climate cooling is more likely to have resulted from increased carbon sequestration via enhanced organic-matter burial and silicate weathering during the earliest part of the OAE, which offset the volcanic CO_2 emissions. Carbon- and lithium-isotope excursions in basal OAE 2 strata support an intensification in both of these potential carbon sinks, consistent with this second model (Blättler et al., 2011; Kuypers et al., 1999; Owens et al., 2018; Pogge von Strandmann et al., 2013).

The shift toward unradiogenic $^{187}Os/^{188}Os_{(i)}$ values just below the base of the OAE 2 level has been widely used to infer that intense LIP volcanism was the cause of the climate warming immediately prior to OAE 2 via volcanic CO_2 emissions, thereby acting as the ultimate trigger of the OAE itself through both the warming and a large-scale release of trace-metal nutrients to the global ocean that stimulated enhanced primary productivity and consequently widespread marine anoxia/euxinia (see Jenkyns, 2010; Robinson et al., 2017; Snow et al., 2005). The OAE sensu stricto is estimated as commencing ~60 kyr after the initiation of intense LIP activity (Du Vivier et al., 2014; Jones et al., 2020), although some other environmental perturbations (such as localized marine redox changes) appear to have begun more rapidly (Jenkyns et al., 2017; Ostrander et al., 2017). Intriguingly however, while $^{187}Os/^{188}Os_{(i)}$ values remain low throughout the PCE strata, they start to become more radiogenic again (from ~0.2 to typically ~0.6) in sediments stratigraphically below the top of the OAE 2 level (e.g., Du Vivier et al., 2014; Du Vivier, Selby, et al., 2015). Such trends suggest that LIP emplacement (and the associated flux of mantle Os to the global ocean) was already declining prior to the end of the environmental crisis, even though a very warm climate was maintained (Robinson et al., 2019). Thus, the extent to which LIP activity played a role in PCE climate cooling via reduced volcanic intensity and the length of time for which the emplacement continued into the later stages of OAE 2 and was able to sustain the persistently warm climate that characterized the second half of the crisis remains less resolved. Crucially, the Os-isotope records of the latest Cenomanian LIP emplacement/activity have not been robustly correlated to paleotemperature trends that document the OAE 2-associated climate changes from the same sites, greatly limiting conjecture regarding causal links between those phenomena, especially for the PCE and later part of OAE 2.

1.2. Study Area and Aims

Here, a new record of seawater Os-isotope changes is presented from a stratigraphic archive of OAE 2 for which paleotemperature data already exist: the bottommost part of the ODP Leg 174AX Bass River core (New Jersey Shelf, NJ, USA; Figure 1). The sedimentary lithology is relatively homogeneous and consists chiefly of very fine-grained (silt-clay) siliciclastics deposited in an inner neritic setting on the northeasternmost continental-shelf margin of the proto-North Atlantic Ocean (Miller et al., 1998). Consequently,

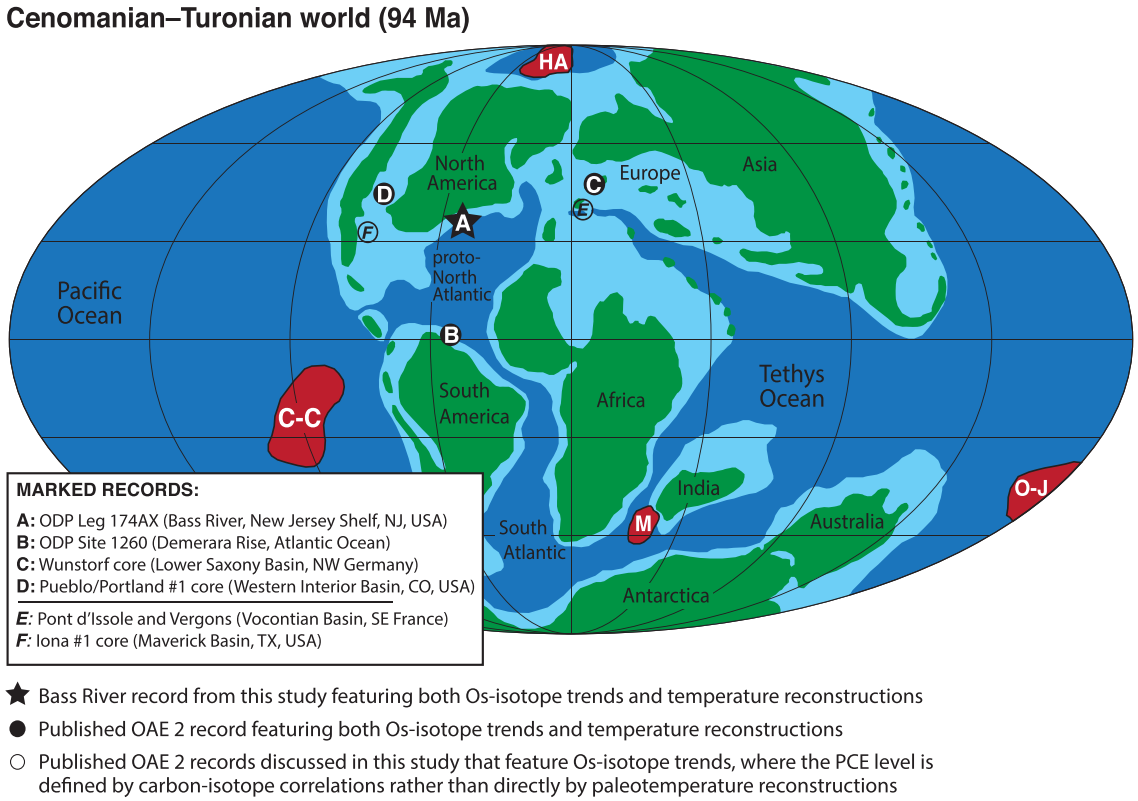

Figure 1. Paleogeographic map of the Cenomanian-Turonian world, indicating the large igneous provinces that have been suggested as having been active during those times, adapted from Percival et al. (2018). The locations of stratigraphic archives of OAE 2 that feature both established Os-isotope trends and paleotemperature data sets, or at least a definition of the PCE level based on carbon-isotope correlations, are as follows: A = ODP Leg 174AX at Bass River (New Jersey Shelf, NJ, USA; van Helmond et al., 2014; this study); B = ODP Site 1260 (Demerara Rise, Atlantic Ocean; Du Vivier et al., 2014; Forster et al., 2007; Turgeon & Creaser, 2008); C = Wunstorf core (Lower Saxony Basin, NW Germany; Du Vivier et al., 2014; van Helmond et al., 2015); D = Pueblo section and Portland #1 core (Western Interior Basin; CO, USA; Desmares et al., 2016; Du Vivier et al., 2014); E = Pont d'Issole and Vergons composite record (Vocontian Basin, SE France; Du Vivier et al., 2014; Jarvis et al., 2011); F = Iona #1 core (Maverick Basin, TX, USA; Sullivan et al., 2020). Note that the Pueblo section and Portland #1 core are distinct records but counted as one stratigraphic archive since they are proximal enough to be directly correlated on a bed-to-bed level. LIPs proposed to have potentially been active during Cenomanian-Turonian times are indicated as follows: C-C = Caribbean-Colombian Plateau; HA = High Arctic LIP; O-J = Greater Ontong-Java Plateau; M = Madagascan Province. See Figure S1 for the paleogeographic positions of other sites referred to in this study but not illustrated on this figure.

anoxic-euxinic conditions did not develop at this location; no lithological change to organic-rich shales or geochemical evidence of severe water-column oxygen depletion is observed (Miller et al., 1998; van Helmond et al., 2014). Nonetheless, the OAE 2 strata are marked by a clear positive CIE of up to 3‰ that spans uppermost Cenomanian-lowermost Turonian sediments 593–580.5 m below the surface (mbs), which is recorded in both bulk organic material ($\delta^{13}C_{org}$) and foraminiferal carbonate ($\delta^{13}C_{carb}$ *Epistomina* and $\delta^{13}C_{carb}$ *Gavelinella*). The base of this CIE is stratigraphically just below the last appearance of planktonic foraminferal *Rotalipora greenhornensis* (*R. greenhornensis*) fossils, broadly consistent with other sites (Bowman & Bralower, 2005; Sugarman et al., 1999; van Helmond et al., 2014; see also Figures 2, 3, and S1 in the supporting information). The precise position of the CTB level itself is less clearly defined due to the relatively poor preservation of ammonites and calcareous microfossils in the siliciclastic sedimentary rocks, including the major marker taxa. A lower limit of 590.6 mbs has been suggested for the boundary based on the limited biostratigraphy (Sugarman et al., 1999). However, a stratigraphically higher placement of this horizon at 581.5 mbs has also been proposed, following correlation of the positive CIE in the Bass River core with other archives of the CTB interval (van Helmond et al., 2014).

SST trends in the paleoenvironment recorded by the Bass River core have been reconstructed using the biomarker-based TEX_{86} paleothermometer and indicate very warm conditions (~37°C) throughout much

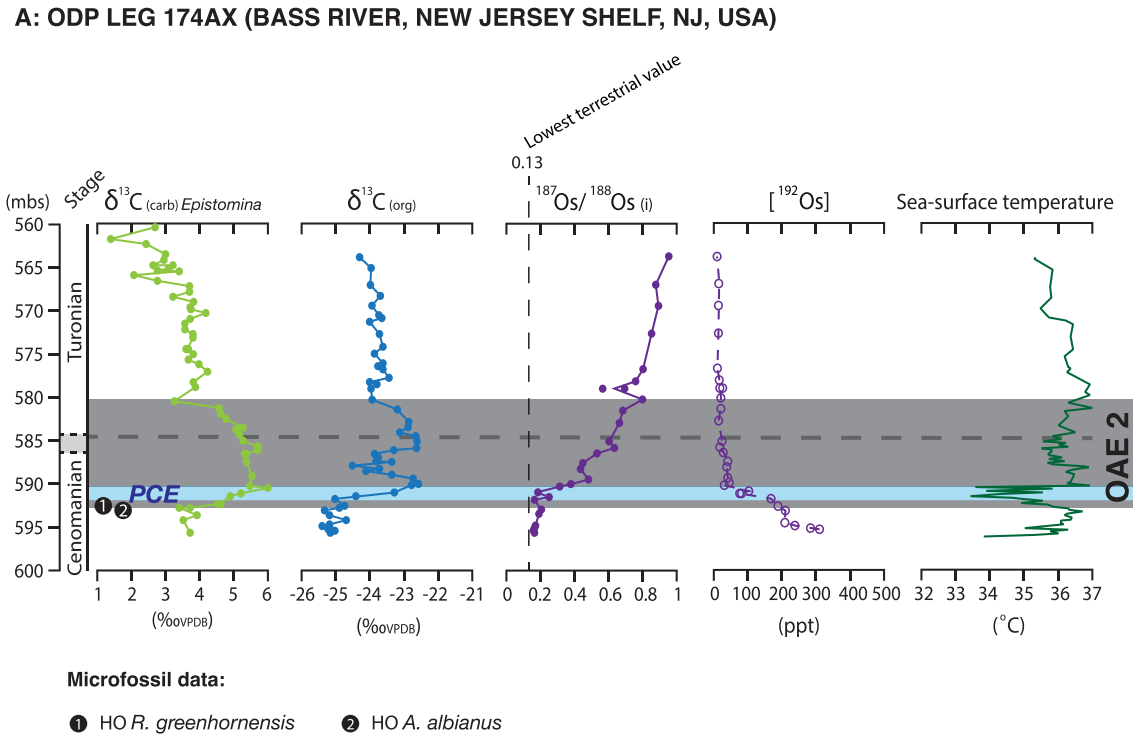

Figure 2. Geochemical data plots for $\delta^{13}C_{carb}$, $\delta^{13}C_{org}$, $^{187}Os/^{188}Os_{(i)}$, [^{192}Os] concentrations, and sea-surface temperatures reconstructed using the biomarker-based TEX_{86} paleothermometer for the ODP Leg 174AX Bass River core. The stratigraphic depth is in meters; stage refers to the stage in geological time. The thick, gray dashed line marks the CTB horizon; the dark gray area indicates the stratigraphic extent of the OAE 2 level; the pale blue area shows the strata that record cooling interpreted as the PCE. The lowest natural terrestrial value of $^{187}Os/^{188}Os$ (0.13; Allègre et al., 1999) is indicated. $\delta^{13}C_{carb}$ data are from Sugarman et al. (1999); $\delta^{13}C_{org}$ data are from van Helmond et al. (2014) and this study; all osmium data are from this study; sea-surface temperature data are from van Helmond et al. (2014). Biostratigraphic information is from Sugarman et al. (1999).

of OAE 2 and subsequent early-Turonian times (van Helmond et al., 2014). A cooling pulse from 37°C to 33°C during the early part of the event is documented between 592 and 590 mbs by the TEX_{86} data and is supported by a spike in boreal-fossil abundance between 591 and 590 mbs, largely consistent with other studies (i.e., Forster et al., 2007; Sinninghe Damsté et al., 2010) and interpreted by van Helmond et al. (2014) as marking the stratigraphic level of the PCE. In this context, a 2‰ negative $\delta^{13}C$ excursion within the overarching positive CIE (between 589.5 and 586 mbs; see Figure 2 and van Helmond et al., 2014), stratigraphically just above the evidence for SST cooling, might be equivalent to the negative CIE broadly correlative with the PCE in several other OAE 2 records.

Thus, establishing a record of seawater Os-isotope changes in the Bass River core and directly correlating it with the previously published evidence for SST changes from that site gives new insights into the temporal and causal relationships between the global climate changes during OAE 2 and the beginning and end of the latest Cenomanian LIP emplacement and volcanism. Because trends in seawater $^{187}Os/^{188}Os_{(i)}$ values for the CTB interval have been robustly correlated stratigraphically across several ocean basins (see Du Vivier et al., 2014; Du Vivier, Selby, et al., 2015), the recorded $^{187}Os/^{188}Os_{(i)}$ trends from the Bass River core also tighten stratigraphic constraints for that site, such as the position of the CTB horizon and whether the negative CIE between 589.5 and 586 mbs is truly equivalent to the excursion associated with the PCE level in other records. Additionally, similar correlations between Os-isotope and paleotemperature data are performed for three records where both data sets exist but have not been previously compared (Figure 1): ODP Site 1260 (Demerara Rise, Atlantic Ocean), the Wunstorf core (Lower Saxony Basin, NW Germany), and the Portland #1 core and nearby Pueblo section (Western Interior Basin, CO, USA). The two Western Interior Basin sites are sufficiently proximal to each other to permit bed-to-bed correlation (see Sageman et al., 2006); thus, they can be treated as a single record when stratigraphically comparing the Os-isotope and paleotemperature trends of the two archives. These comparisons allow any differences in the timing

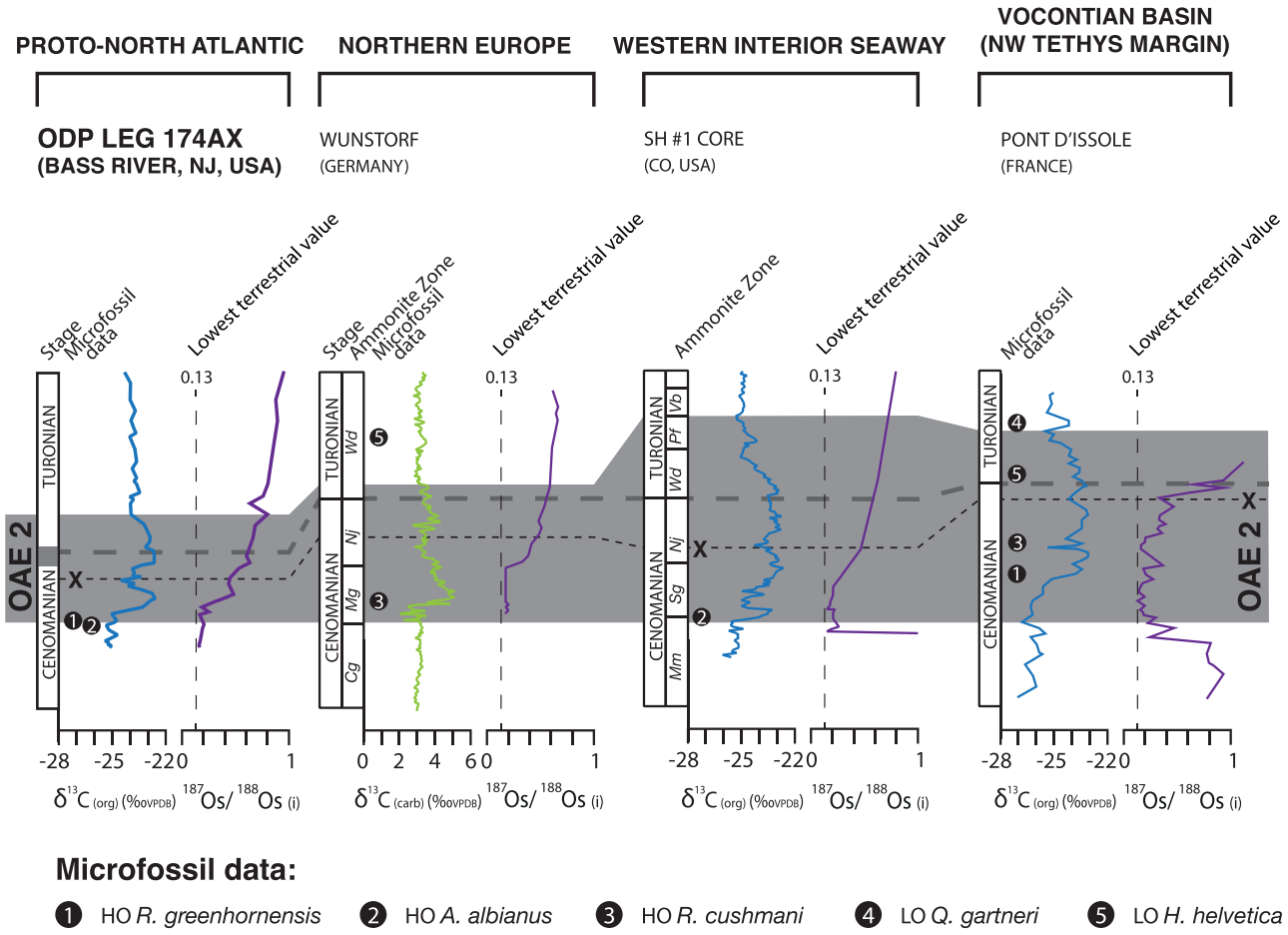

Figure 3. Correlation of the ODP Leg 174AX Bass River stratigraphic archive of OAE 2 with those from northern Europe, the Western Interior Seaway, and the Vocontian Basin, based on carbon-isotope trends and ammonite and microfossil biostratigraphy. The geographic locations of the SH #1 core are approximately the same as that of Pueblo/Portland #1 core in Figure 1. Stage refers to the stage in geological time. *Cg*, *Mg*, *Nj*, *Wd*, *Mm*, *Sg*, *Pf*, and *Vb* refer to the *C. guerangeri*, *M. geslinianum*, *N. juddii*, *W. devonense*, *M. mosbyense*, *S. gracile*, *P. flexuosum*, and *V. birchbyi* ammonite zones, respectively. The thick, gray dashed line marks the CTB horizon; the thin, black dashed line (X) marks a postulated correlation between negative CIEs in the *N. juddii* ammonite zone just below the CTB; the dark gray area indicates the stratigraphic extent of the OAE 2 level. The lowest natural terrestrial value of $^{187}Os/^{188}Os$ (0.13; Allègre et al., 1999) is indicated. Pueblo and the Portland #1 core are directly correlated with each other by bed number. Carbon-isotope and biostratigraphic data are sourced as follows: ODP Leg 174AX Bass River from Sugarman et al. (1999); van Helmond et al. (2014) and this study; Wunstorf from Voigt et al. (2008); SH #1 from Jones et al. (2019); Pont d'Issole from Jarvis et al. (2011). Osmium-isotope data are sourced as follows: ODP Leg 174AX Bass River from this study; Wunstorf, and Pont d'Issole from Du Vivier et al. (2014); SH #1 from Jones et al. (2020).

of the PCE cooling or return to warm conditions across locations spanning the northern and equatorial proto-North Atlantic, the central Western Interior Seaway, and northern European area to be established. Confirming whether there was a geographical pattern in the postulated diachroneity of cooling during the PCE, how those differences were related to the latest Cenomanian LIP formation, and determining for how long LIP volcanism continued into OAE 2 and was able to sustain the documented warm temperatures advances our understanding of the climate changes and associated environmental perturbations during one of the most severe global crises of the Mesozoic Era.

2. Methods

Concentrations and isotopic compositions of Re and Os were determined by combining isotope dilution with negative thermal ionization techniques using a ThermoScientific Triton at the University of Durham (UK). Sample preparation was carried out using Carius-tube digestion with $Cr^{VI}O_3$-H_2SO_4, with

Os purification achieved following established solvent extraction (by $CHCl_3$) and microdistillation methods (Selby & Creaser, 2003). Rhenium purification utilized single-bead anion chromatography, following treatment with NaOH and acetone (Cumming et al., 2013; Selby & Creaser, 2003). Procedural blanks were 19.4 ± 2.0 pg for Re and 0.07 ± 0.01 pg for Os, with a $^{187}Os/^{188}Os$ ratio of 0.16 ± 0.05 (1σ; $n = 4$). In-house standards were used to monitor analytical reproducibility (see Nowell et al., 2008, and supplementary information in Du Vivier et al., 2014). Mean standard $^{187}Os/^{188}Os$ (50 pg DROsS) and $^{187}Re/^{185}Re$ (125 pg ReSTD) values generated during the sample analyses were 0.16075 ± 0.00016 (1σ; $n = 23$) and 0.59820 ± 0.00082 (1σ; $n = 19$), respectively, consistent with running averages for the lab. Full details of measurements for all samples, in-house standards, and blanks are reported in the supplementary data tables published in PANGAEA (see Data Availability Statement below).

Ten additional Bass River sedimentary rock samples between 580 and 592 mbs were analyzed for $\delta^{13}C_{org}$ on a Thermo Delta-V coupled to an EA Isolink CN mass spectrometer at Utrecht University (Netherlands), following decarbonation via the method outlined in van Helmond et al. (2014). A graphite-quartz mixture calibrated against several international reference materials (USGS-24, NBS-22, IAEA-CH-3, and IAEA-CH-7) was used as an in-house standard, with a nicotinamide sample measured as a further control. The average value determined for the in-house standard measurements was −26.77 ± 0.20‰ (1σ; $n = 6$), consistent with expected values for the lab (−26.68‰). The new data are combined with the previous 42-sample data set of van Helmond et al. (2014) and reported as per mil (‰) relative to the Vienna Peedee belemnite standard (see data tables published in PANGAEA).

3. Results

The base of the studied interval (below 591 mbs) features concentrations between 79 and 314 ppt of "common" ^{192}Os, which are markedly higher than those for the remainder of the investigated strata (10–45 ppt ^{192}Os; Figure 2). The Os-enriched samples below 591 mbs also feature a very unradiogenic initial isotopic composition ($^{187}Os/^{188}Os_{(i)} = 0.16–0.26$) following age correction to 94 Ma (Figure 2). From 591 mbs upward, the recorded $^{187}Os/^{188}Os_{(i)}$ values rise toward levels indicative of an increasingly radiogenic seawater composition, reaching ~0.5 just above 590 mbs, ~0.6 by 585 mbs, and 0.8 by 580 mbs (equivalent to the top of the OAE 2 strata as defined by the positive CIE excursion). Above the OAE 2 level, this rise in the recorded $^{187}Os/^{188}Os_{(i)}$ values continues, albeit more gradually, eventually exceeding 0.9 in the topmost studied samples (Figure 2). As with most other OAE 2 records, rhenium contents show a lower degree of variability than do Os concentrations (0.88–4.48 ppb), although there is a trend toward lower Re abundances higher in the studied stratigraphic interval.

The new $\delta^{13}C_{org}$ data determined from Bass River samples for this study are used to increase the resolution of the 2014 carbon-isotope curve from that site (van Helmond et al., 2014), as well as to confirm and extend previously observed trends. The stratigraphic extent of the positive CIE (and consequently the OAE 2 level) is unchanged based on the new data. However, a negative CIE from −22.5‰ to −24.5‰ within the overarching positive (between 589.5 and 586 mbs) that was previously indicated by only a single data point is now much more clearly defined by nine samples (Figure 2). This excursion in $\delta^{13}C_{org}$ might also be matched by a shift $\delta^{13}C_{carb}$ ratios of *Epistomina* fossils between 590.5 and 586.3 mbs, although the much lower magnitude of the $\delta^{13}C_{carb}$ shift means that the conclusion of a common cause for the two CIEs can only be made tentatively.

4. Discussion

4.1. OAE 2 Os-Isotope Stratigraphy of the Bass River Core

The presence of ^{192}Os-enriched samples that record unradiogenic $^{187}Os/^{188}Os_{(i)}$ values in the lowest OAE 2 and pre-OAE strata (below 591 mbs) of the Bass River core is consistent with previous Cenomanian-Turonian Os data sets and is likewise interpreted as indicating a major flux of mantle-derived Os to the global ocean during LIP emplacement prior to and during the early part of OAE 2. However, the base of the Os enrichment and shift to unradiogenic $^{187}Os/^{188}Os_{(i)}$ compositions (reported just below the OAE level in previous studies; e.g., Du Vivier et al., 2014; Jones et al., 2020; Sullivan et al., 2020; Turgeon & Creaser, 2008) is not documented from the stratigraphic interval of the Bass River core studied

here. Therefore, based on the global $^{187}Os/^{188}Os_{(i)}$ profile for just prior to OAE 2, the stratigraphically lowermost samples investigated in this study must have been deposited after the onset of intense latest-Cenomanian LIP emplacement, with sediments recording that time interval potentially preserved below the bottom of the drilled Bass River core (base 596.3 mbs).

The return toward a pre-event Os-isotope seawater composition during the later stages of the OAE is clearly documented in the Bass River core, with recorded $^{187}Os/^{188}Os_{(i)}$ trends that are highly comparable to those of previously studied sites, particularly Wunstorf and the Western Interior Seaway archives (e.g., Du Vivier et al., 2014; Jones et al., 2020; Sullivan et al., 2020; see also Figures 3 and 4). The similarity in recorded $^{187}Os/^{188}Os_{(i)}$ trends from this study to previously published data sets from sites spanning other marine basins, combined with the open-marine setting of the New Jersey Shelf facing the proto-North Atlantic Ocean, strongly suggests that the Bass River core does not record a hydrographically restricted paleoenvironment. Thus, this archive should reliably document the changes in global-ocean seawater Os-isotope composition that took place during OAE 2. In this case, the Bass River Os-isotope stratigraphy can both be utilized as a robust chemostratigraphic tool to correlate the New Jersey Shelf strata with other OAE 2 records and illustrate the temporal relationship between latest- Cenomanian LIP emplacement and climate changes on the New Jersey Shelf during that time interval. Thus, the turning point in $^{187}Os/^{188}Os_{(i)}$ values within the OAE 2 level, where they begin to return toward pre-OAE Os-isotope ratios, can be used as a stratigraphic anchor point in Cenomanian-Turonian stratigraphic archives (see Os-isotope chronology of Du Vivier, Selby, et al., 2015), together with both the CTB level and globally recorded features of the positive CIE.

Based on a whole OAE 2 CIE duration of 430–450 kyr (derived from the Wunstorf core; Voigt et al., 2008), van Helmond et al. (2014) calculated a deposition rate of ~3 cm/kyr for the lowest part of the Bass River core. Sedimentation on the New Jersey Shelf was likely broadly constant during OAE 2, based on both the relatively homogenous lithology and the assumed control on sediment deposition by basin subsidence (which would be expected to have changed little over the timescales of OAE 2). Thus, for a ~220 kyr time interval recorded by sediments deposited between the CTB and the turning point in $^{187}Os/^{188}Os_{(i)}$ (also derived from the Wunstorf core; Voigt et al., 2008), a ~3 cm/kyr sedimentation rate would place the CTB level in the Bass River core at 584.5 mbs. Alternatively, an 800–1,000 kyr duration for the whole of the OAE 2 CIE (as determined for most Western Interior Seaway records; e.g., Eldrett et al., 2015; Jones et al., 2020; Meyers et al., 2012; Sageman et al., 2006; Sullivan et al., 2020) yields a deposition rate of 1.25–1.56 cm/kyr for the Bass River core OAE 2 strata. In this case, utilizing a time interval of ~350–400 kyr for the sediments between the CTB and turning point in $^{187}Os/^{188}Os_{(i)}$ values of those Western Interior Seaway sites (Du Vivier et al., 2014; Du Vivier, Selby, et al., 2015; Jones et al., 2020; Sullivan et al., 2020) places the CTB level between 586.7 and 584.8 mbs in the Bass River core. Consequently, combining global Os-isotope stratigraphy with cyclostratigraphic age models of OAE 2 records around the world allows the CTB level to be constrained between 586.7 and 584.5 mbs in the Bass River core and probably toward the upper end of that range based on similar site-to-site carbon-isotope correlations (Figures 2 and 3). Recorded $^{187}Os/^{188}Os_{(i)}$ values of ~0.6 for samples between 586 and 583 mbs in the Bass River core are comparable to seawater Os-isotope ratios recorded at the CTB horizon at other sites and may further support this placement. This slightly revised position of the CTB level in the Bass River core is broadly consistent with, but slightly lower than, the estimate of van Helmond et al. (2014) but is significantly higher than the lower limit postulated by Sugarman et al. (1999) based on (admittedly limited) planktonic foraminiferal and calcareous nannofossil biostratigraphic information.

Furthermore, the negative $\delta^{13}C_{org}$ excursion between 589.5 and 586 mbs, which looks superficially similar to the negative CIE associated with the PCE level at many other sites globally, is stratigraphically too high with respect to the $^{187}Os/^{188}Os_{(i)}$ turning point to actually be equivalent to that excursion (Figure 3). The CIE associated with the PCE (correlative with the highest appearance of *R. cushmani* fossils) is clearly correlative with very unradiogenic $^{187}Os/^{188}Os_{(i)}$ ratios at all of Wunstorf, Pont d'Issole, and the SH #1, Iona, and Portland cores. By contrast, the pronounced negative CIE within the overarching positive shift in the Bass River core occurs in strata that record the rise in $^{187}Os/^{188}Os_{(i)}$ back toward radiogenic values. Consequently, the negative $\delta^{13}C_{org}$ excursion in the Bass River core is more likely equivalent to a subsidiary negative CIE documented just below the CTB in some, though not all, records of OAE 2 (e.g., Pont d'Issole and Clot Chevalier, SE France; Wunstorf core, Germany; SH #1 core, CO, USA; and Oued Mellegue, Tunisia;

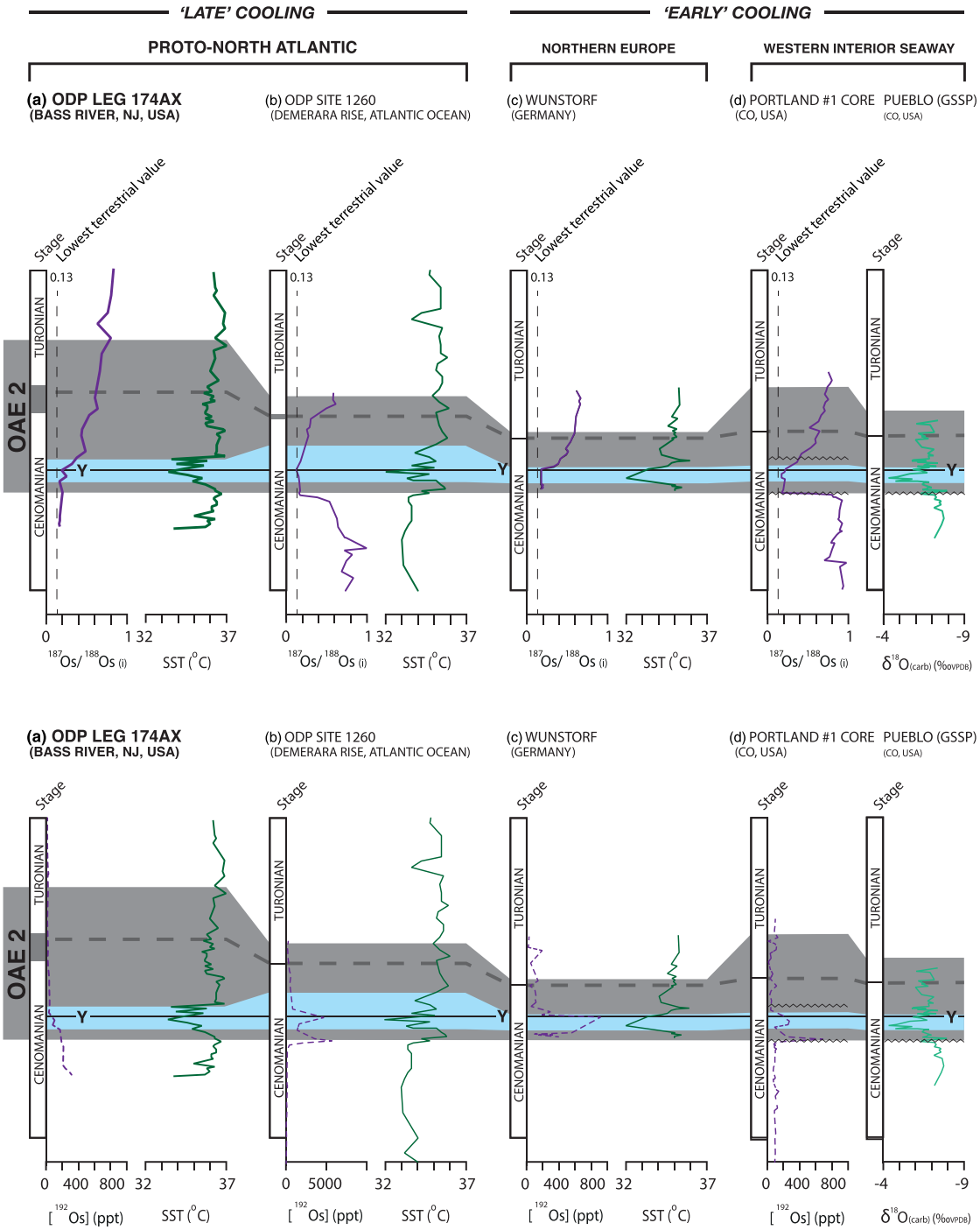

Figure 4. Correlation of osmium-isotope and paleotemperature trends from stratigraphic archives of OAE 2. Pueblo and the Portland #1 core are directly correlated with each other by bed number. For the Bass River core, ODP Site 1260, and Wunstorf, paleotemperature trends are directly reconstructed from TEX_{86} proxy data; at Pueblo, evidence for cooling is from combined oxygen-isotope data and foraminiferal morphology changes, which when taken together are assumed to reflect relative changes in temperature, rather than salinity variations or diagenetic processes (Desmares et al., 2016). The thin black line Y marks the turning point in recorded trends of $^{187}Os/^{188}Os_{(i)}$ values, assumed to be time equivalent for all Cenomanian-Turonian records of open-marine environments. The thick, gray dashed line marks the CTB horizon; the dark gray area indicates the stratigraphic extent of the OAE 2 level; the pale blue area shows the strata that record cooling interpreted as the PCE. The lowest natural terrestrial value of $^{187}Os/^{188}Os$ (0.13; Allègre et al., 1999) is indicated. Stage refers to the stage in geological time. Osmium-isotope data are sourced as follows: ODP Leg 174AX Bass River from this study; ODP Site 1260 from Turgeon and Creaser (2008) and Du Vivier et al. (2014); Wunstorf and Portland #1 core from Du Vivier et al. (2014). Sea-surface temperature data are sourced as follows: ODP Leg 174AX Bass River from van Helmond et al. (2014); ODP Site 1260 from Forster et al. (2007); and Wunstorf from van Helmond et al. (2015). Pueblo oxygen-isotope data are from Desmares et al. (2016).

Caron et al., 2006; Falzoni et al., 2016; Gale et al., 2018; Jarvis et al., 2011; Jones et al., 2019; Nederbragt & Fiorentino, 1999; Voigt et al., 2008; see also Figures 3 and S1), and which also correlates with trends of increasing $^{187}Os/^{188}Os_{(i)}$ values in all of the Wunstorf, Pont d'Issole, and SH #1 records (Figure 3). However, if the negative $\delta^{13}C_{org}$ excursion in the Bass River core is indeed equivalent to such a subsidiary CIE, it is not clear why no stratigraphically lower negative excursion in $\delta^{13}C_{org}$ is preserved between 592 and 590 mbs, correlative with the evidence for SST cooling. The presence of a stratigraphic hiatus at that level cannot be excluded, but there is no clear evidence for such a break in sediment deposition. Interestingly, negative CIEs in benthic foraminiferal calcite have been reported from between 592 and 590 mbs, although they likely result from diagenetic alteration, at least to some degree (Bowman & Bralower, 2005; Sugarman et al., 1999).

4.2. Timing of OAE 2 Paleotemperature Changes Compared to $^{187}Os/^{188}Os_{(i)}$ Fluctuations and LIP Activity

As noted above, the $^{187}Os/^{188}Os_{(i)}$ stratigraphic anchor points can also be utilized to assess the temporal relationships between recorded paleotemperature changes, carbon-cycle perturbations, and LIP emplacement during OAE 2. Figure 4 compares the stratigraphic relationships between $^{187}Os/^{188}Os_{(i)}$ and paleotemperature trends of both the Bass River core and the previously published data sets from ODP Site 1260, the Wunstorf core, and the Portland #1 core/Pueblo section. Only one of the four presented archives (ODP Site 1260) features stratigraphically complete trends that record both the onset of climate warming associated with OAE 2 and the initiation of LIP emplacement as recorded by the shift in $^{187}Os/^{188}Os_{(i)}$ values to ~0.2. While a correlation between the evidence of pre-OAE warming and the start of LIP activity at that site supports the accepted causal link between the two phenomena, further Os-isotope and paleotemperature studies from the basal OAE strata at other locations are needed to verify a global-scale synchronicity between these phenomena.

However, assuming that the turning point in recorded $^{187}Os/^{188}Os_{(i)}$ from lower OAE 2 strata is globally time equivalent (see above), useful observations can still be made from these site-to-site comparisons regarding how SSTs developed with respect to LIP activity (and the global-ocean Os-isotope composition) during the PCE and later part of OAE 2. Most strikingly, the SST minima documented in sediments from the Wunstorf core and Pueblo lie significantly stratigraphically below the turning point in $^{187}Os/^{188}Os_{(i)}$ back toward radiogenic values, whereas the lowest temperatures reconstructed from the Bass River and ODP Site 1260 records are documented at or even slightly above that level (Figure 4). Moreover, SSTs for Wunstorf and Pueblo had returned to almost pre-PCE conditions by the time that seawater $^{187}Os/^{188}Os$ ratios began to increase; whereas at Bass River and ODP Site 1260, the return to warmer conditions did not begin until after the seawater $^{187}Os/^{188}Os$ composition had already become more radiogenic. Thus, both the cooling to the coldest temperatures during the PCE and the return to warm conditions afterward appear to have taken place noticeably later at the two Atlantic locations than in the central Western Interior Seaway and northern Europe. This pattern supports the hypothesis of regional diachroneity in the PCE climate change proposed by O'Connor et al. (2020), who also noted the apparent “earliness” of the cooling in parts of Europe and the Western Interior Seaway.

Similar correlations can be attempted for Pont d'Issole (Vocontian Basin, SE France) and the Iona #1 core (Maverick Basin, TX, USA), for which the turning points in $^{187}Os/^{188}Os_{(i)}$ values are above the top of and in the middle of the PCE level, respectively (see Figure S2). This observation might indicate that SST cooling and/or water-column reoxygenation took place relatively early during OAE 2 in the Vocontian Basin, as for nearby northern Europe. In contrast, the PCE apparently occurred later in the Maverick Basin at the southern end of the Western Interior Seaway, more akin to the timing of cold conditions in the proto-North Atlantic realm than to the central part of the Western Interior Seaway. However, such interpretations can only be made tentatively for these two sites, as the stratigraphic placement of the PCE level in those records is not based on direct evidence of cooling temperatures at those locations, but primarily via carbon-isotope correlations with other OAE 2 archives such as Eastbourne (Anglo-Paris Basin, UK). While the geographical proximity of the Ango-Paris and Vocontian basins and the recorded southward migration of cool-water belemnites do support synchronous cooling across those two locations, there is no guarantee that cold conditions developed at the same time in the Anglo-Paris and Maverick basins.

If northern Europe and the central Western Interior Seaway were indeed among the earliest locations to experience PCE cooling, then the temperature declines recorded at Wunstorf and Pueblo should have occurred during or soon after the reduction in atmospheric pCO_2 thought to have triggered the cold conditions (Jarvis et al., 2011; Sinninghe Damsté et al., 2010). In this context, it is notable that the SST drops at both Pueblo and Wunstorf are recorded in strata with an elevated ^{192}Os concentration (Figure 4). Assuming that peaks in ^{192}Os do reflect pulses in volcanic activity, as previously suggested (Jones et al., 2020; Sullivan et al., 2020; Turgeon & Creaser, 2008), this correlation implies that intense volcanic activity was taking place at the time of the earliest known PCE cooling. Consequently, based on direct correlation of Os-isotope and paleotemperature data, the model of PCE cooling caused by elevated carbon sequestration appears to be more plausible than the alternative scenario whereby volcanic quiescence led to a reduction in CO_2 emissions. This conclusion is reinforced by the placement of the PCE level in the Iona #1 core stratigraphically above the evidence for cooling at Pueblo and in the Wunstorf core (relative to the $^{187}Os/^{188}Os_{(i)}$ turning point), indicating that the PCE level postulated for the Iona #1 core likely does not record the time of the earliest drop in temperatures across the globe (see above). As noted in section 1, rates of both organic-carbon burial and silicate weathering (the most probable carbon sinks to have strongly influenced atmospheric pCO_2) likely increased significantly during the earliest part of OAE 2 (Blättler et al., 2011; Jenkyns, 2010; Owens et al., 2018; Pogge von Strandmann et al., 2013). Thus, both processes would have been capable of acting as efficient sinks of CO_2 from the ocean-atmosphere system, leading to the cooling that characterized the PCE.

Continued LIP volcanism could have caused the return to a globally warm climate that marked the end of the PCE, likely aided by a decrease in organic-carbon burial in locally reoxygenated marine environments that acted to reduce CO_2 drawdown. The coeval return of widespread marine anoxia/euxinia may have been stimulated both by the warming and a proposed micronutrient perturbation that took place during the PCE (Sweere et al., 2018). However, the observation that the turning point in $^{187}Os/^{188}Os_{(i)}$ back toward higher values is found within or just above the PCE level at all four of the correlated sites shown in Figure 4 indicates that LIP emplacement (and, presumably, the associated volcanism) started to decline around the time that the cooling pulse ended. Thus, while volcanic CO_2 emissions may have helped stimulate the temperature rise at the end of the PCE, they were unlikely to have played much of a role in sustaining the persistently warm conditions prevalent through the second half of OAE 2.

Maintaining a globally warm climate throughout the second part of OAE 2, even as CO_2 emissions were falling, would have required the global carbon sinks to have also been muted during that time interval (Robinson et al., 2019). Although there are several different age models for the duration of the OAE (e.g., Eldrett et al., 2015; Ma et al., 2014; Sageman et al., 2006; Voigt et al., 2008), all of them agree that the second half of OAE 2 lasted for hundreds of kiloyears after the PCE. While carbon sequestration via organic-matter burial might have been lower during the second half of the OAE than at its onset, organic-carbon deposition must still have been relatively high (at least in some areas) to maintain relatively high sedimentary $\delta^{13}C$ values across strata recording hundreds of kiloyears of time (e.g., Arthur et al., 1988; Jarvis et al., 2011; Tsikos et al., 2004). Consequently, the reduction in carbon sequestration during the second half of OAE 2 was more likely linked to a significant fall in silicate weathering rates, as previously postulated (Robinson et al., 2019). In this context, it is noteworthy that most studied archives feature significantly lower sedimentary $^{187}Os/^{188}Os_{(i)}$ values in and above uppermost OAE 2 strata compared to sediments below the event level. This pattern supports a less radiogenic oceanic Os-isotope composition post-OAE 2 than prior to it, potentially resulting from a reduced runoff of continental material.

Intense silicate weathering during the earliest part of the OAE, which subsequently declined as the event progressed, is further supported by lithium-isotope trends from Eastbourne (Pogge von Strandmann et al., 2013; see also Figure 5). Shifts to isotopically lighter lithium- and calcium-isotope ratios at Raia de Pedale (Italy) and South Ferriby (UK) both suggest a significant pulse of weathering during the latest part of the OAE as well (Blättler et al., 2011; Pogge von Strandmann et al., 2013), although positive excursions in calcium isotopes have also been noted for some OAE 2 sites and linked to a change in oceanic carbonate content caused by increasingly acidic marine conditions (Du Vivier, Jacobson, et al., 2015). However, basal OAE 2 strata are missing from at least the South Ferriby site, and stratigraphically correlating Raia de Pedale with other OAE 2 archives is nontrivial.

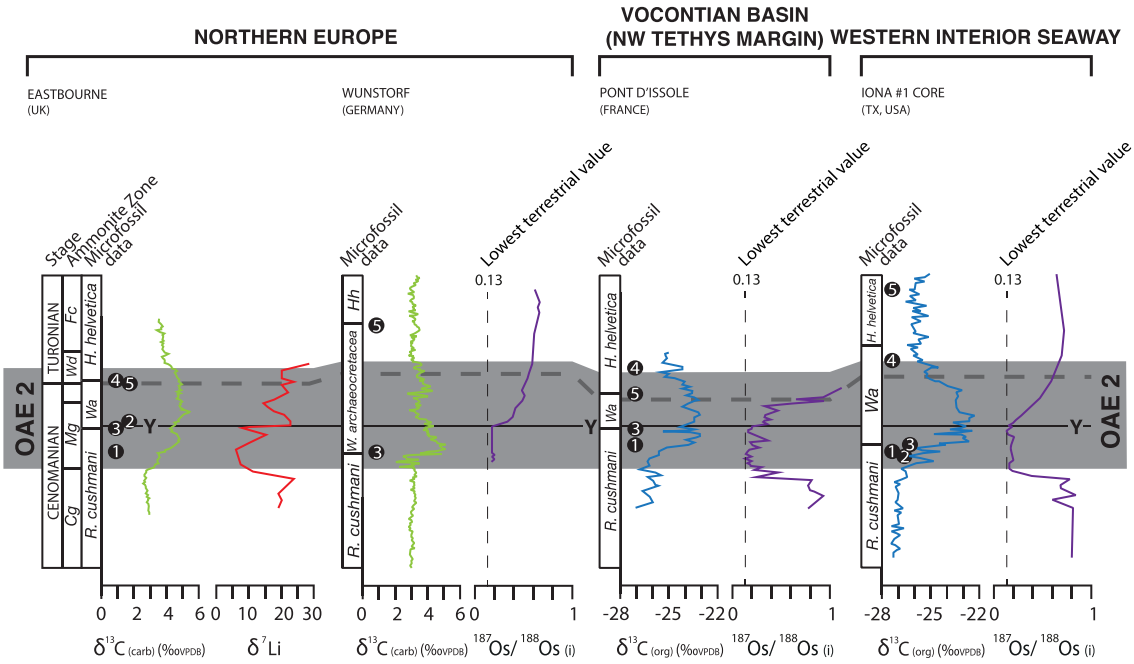

Figure 5. Correlation of osmium- and lithium-isotope trends from the stratigraphic archives of OAE 2. The geographic location of Eastbourne is shown in Figure S1. The thick, gray dashed line marks the CTB horizon; the thin, black line (Y) marks the turning point in recorded trends of $^{187}Os/^{188}Os_{(i)}$ values; the dark gray area indicates the stratigraphic extent of the OAE 2 level. Ammonite-zone abbreviations as for Figure 3; for microfossil zones, *Wa* and *Hh* indicate *W. archaeocretacea* and *H. helvetica*, respectively. Stage refers to the stage in geological time. The lowest natural terrestrial value of $^{187}Os/^{188}Os$ (0.13; Allègre et al., 1999) is indicated. Osmium-isotope data are sourced as follows: Wunstorf and Pont d'Issole from Du Vivier et al. (2014); Iona #1 core from Sullivan et al. (2020). Eastbourne lithium-isotope data are from Pogge von Strandmann et al. (2013). Carbon-isotope and biostratigraphic information as for Figure 3, except for Eastbourne (from Tsikos et al., 2004) and the Iona #1 core (from Eldrett et al., 2015).

Assuming that silicate weathering rates did indeed fall during the later stages of OAE 2 and that the Eastbourne lithium-isotope trends are the most globally representative archive of those changes, an intriguing observation is that lithium-isotope values at Eastbourne return sharply toward pre-event compositions in the lowermost part of the *W. archaeocretacea* foraminiferal zone, broadly correlative with the level of the turning point in $^{187}Os/^{188}Os_{(i)}$ values back toward radiogenic compositions at Wunstorf, Pont d'Issole, and the SH #1, Iona, and Portland cores (see Figure 5). Thus, it appears that the intensity of silicate weathering began to drop around the same time that LIP volcanism and the interaction of those newly erupted basalts with the global ocean began to decline. A coeval onset in the waning of those two processes would support a major contribution toward global silicate weathering during OAE 2 from the erosion of juvenile LIP basalts (which are known to be highly weatherable; see Dessert et al., 2001), consistent with the original hypothesis of Pogge von Strandmann et al. (2013). While a contribution from the erosion of continental material toward silicate weathering during OAE 2 cannot be ruled out, continental weathering rates are highly dependent on global temperatures (Kump et al., 2000). Consequently, the comparably warm conditions during the earliest and later parts of OAE 2 are not consistent with a reduction in continental weathering as the OAE progressed. Indeed, it has been proposed that enhanced hydrological cycling and terrestrial runoff took place on the New Jersey Shelf during the later stages of OAE 2 (van Helmond et al., 2014), although the increased weathering in that area may have only been a local phenomenon.

Thus, the erosion of juvenile LIP basalts was probably the greater contributor toward silicate weathering during OAE 2, either through the breakdown of exposed LIP rocks or submarine alteration of oceanic-plateau basalts. At least some parts of the Caribbean-Colombian Plateau are known to have become emergent above the sea surface (Buchs et al., 2018), and the rapid weathering of such rocks in the Central Atlantic Magmatic Province has been proposed as a significant CO_2 sink during the Triassic-Jurassic transition (Schaller et al., 2012). Submarine-basalt alteration has also been advocated as a significant sink within the modern carbon cycle, although this remains debated (see Alt & Teagle, 1999; Berner, 2004). In either

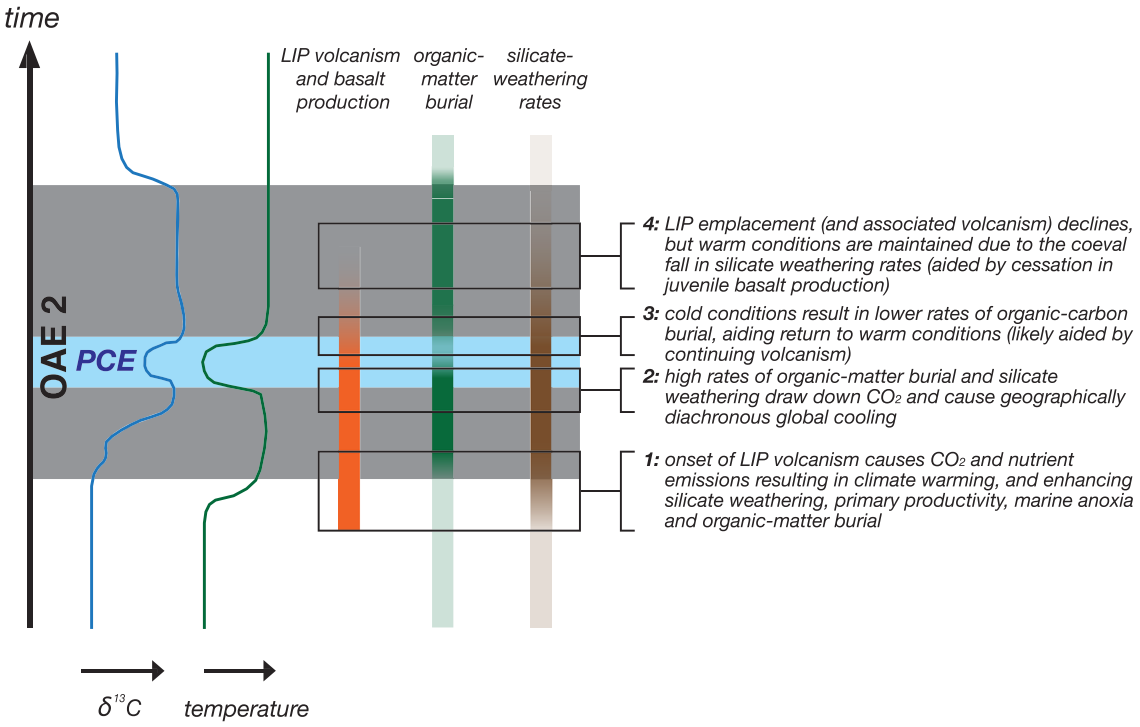

Figure 6. Timeline of processes influencing global temperatures during OAE 2, with idealized curves of seawater $\delta^{13}C$ and sea-surface temperature, and schematic indications of the qualitative trends in rates of LIP volcanic activity, organic-matter burial, and silicate weathering (bolder color = higher rate). The dark gray area indicates the duration of OAE 2; the pale blue area shows the generalized duration of the Plenus Cold Event.

case, both processes would have been greatly enhanced while LIPs were volcanically active during their emplacement and would have rapidly declined once LIP emplacement started to wane around the end of the PCE. This decline would have weakened the influence of silicate weathering as a carbon sink and aided the continuation of a very warm global climate throughout the second part of OAE 2 despite the reduction in volcanic CO_2 emissions and resumption of high rates of organic-matter burial (see Figure 6). Clearly, the relationship between LIP formation and environmental perturbations during OAE 2 was highly complex following the rise in global temperatures when the volcanism began, incorporating both volcanic emissions of CO_2 and sequestration of that greenhouse gas during silicate weathering of newly erupted basalts.

5. Conclusions

This study has presented a new Os-isotope record of LIP emplacement from the OAE 2 archive of the ODP Leg 174AX Bass River core and performed the first direct correlation of those trends with evidence for coeval sea-surface temperature changes from the same site, including the cooling associated with the PCE and the return to sustained warm conditions during the second half of the OAE. The changes in seawater Os-isotope composition recorded from the Bass River core are consistent with those documented from other marine basins around the world, aiding stratigraphic constraints on that record, and are likewise interpreted as having been caused by a major flux of mantle Os to the global ocean from one or more igneous provinces that were emplaced during the latest Cenomanian. Comparing four OAE 2 archives (including the Bass River core) featuring both Os-isotope records of LIP emplacement and paleotemperature data that can be directly correlated and utilizing the globally documented trends in seawater Os-isotope compositions during OAE 2 allow the temporal and causal relationships between LIP activity and global climates during the OAE to be evaluated. The comparisons highlight that the earliest cooling coincided with a pulse of LIP volcanism, suggesting that the shift to colder climates was more likely to have been caused by increased carbon sequestration than to have occurred because of a spell of volcanic quiescence. Rates of LIP emplacement are also shown to have started declining before the midpoint of OAE 2, supporting a reduction in silicate

weathering rates rather than continued volcanism as the major cause of a persistently warm climate throughout the second half of the OAE, with the cessation of LIP eruptions and production of readily eroded juvenile basalts potentially key in this regard. Moreover, comparisons of the four sites support previous hypotheses of a regional diachroneity in the sea-surface cooling associated with the PCE, likely resulting from globally heterogeneous heat transfer by oceanic/atmospheric circulation and/or other regional controls. Taken together, these findings emphasize a profoundly nuanced relationship between latest Cenomanian LIPs and the global climate during OAE 2. Future studies are needed to further investigate the complexities of LIP-environmental interactions during other major events in Earth's history by directly correlating records of paleotemperature changes to robust proxies of volcanism.

Data Availability Statement

Geochemical data are available in the repository PANGAEA (https://doi.org/10.1594/PANGAEA.920743).

Acknowledgments
We thank Ian Jarvis and one anonymous reviewer for their constructive feedback that has improved this manuscript. We greatly appreciate the laboratory assistance given by Geoff Nowell, Chris Ottley, Antonia Hofmann, and Arnold van Dijk. We gratefully acknowledge the TOTAL Endowment Fund and the Dida Scholarship from CUG Wuhan (D. S.), the Netherlands Earth System Science Center (N. A. G. M. v. H.), the Research Foundation – Flanders (FWO grant no. 12P4519N to L. M. E. P. and EOS ID 30442502 to S. G.), Vrije Universiteit Brussel Strategic Research, and Université de Lausanne (L. M. E. P.) for funding.

References

Allègre, C. J., Birck, J. L., Capmas, F., & Courtillot, V. (1999). Age of the Deccan traps using ^{187}Re–^{187}Os systematics. *Earth and Planetary Science Letters*, *170*(3), 197–204. https://doi.org/10.1016/S0012-821X(99)00110-7

Alt, J. C., & Teagle, D. A. (1999). The uptake of carbon during alteration of ocean crust. *Geochimica et Cosmochimica Acta*, *63*(10), 1527–1535. https://doi.org/10.1016/S0016-7037(99)00123-4

Arthur, M. A., Dean, W. E., & Pratt, L. M. (1988). Geochemical and climatic effects of increased marine organic carbon burial at the Cenomanian/Turonian boundary. *Nature*, *335*(6192), 714–717. https://doi.org/10.1038/335714a0

Arthur, M. A., & Premoli-Silva, I. (1982). Development of widespread organic-rich strata in the Mediterranean Tethys. In S. O. Schlanger & M. B. Cita (Eds.), *Nature and origin of Cretaceous carbon-rich facies* (pp. 7–54). London: Academic.

Barclay, R. S., McElwain, J. C., & Sageman, B. B. (2010). Carbon sequestration activated by a volcanic CO_2 pulse during Ocean Anoxic Event 2. *Nature Geoscience*, *3*(3), 205–208. https://doi.org/10.1038/NGEO757

Berner, R. A. (2004). *The Phanerozoic carbon cycle* (p. 150). New York: Oxford University Press.

Blättler, C. L., Jenkyns, H. C., Reynard, L. M., & Henderson, G. M. (2011). Significant increases in global weathering during Oceanic Anoxic Events 1a and 2 indicated by calcium isotopes. *Earth and Planetary Science Letters*, *309*(1–2), 77–88. https://doi.org/10.1016/j.epsl.2011.06.029

Bond, D. P., & Wignall, P. B. (2014). *Volcanism, impacts, and mass extinctions: Causes and effects*, *Geological Society of America Special Papers* (Vol. 505, pp. 29–55). Geological Society of America. https://doi.org/10.1130/2014.2505(02)

Bowman, A. R., & Bralower, T. J. (2005). Paleoceanographic significance of high-resolution carbon isotope records across the Cenomanian–Turonian boundary in the Western Interior and New Jersey coastal plain, USA. *Marine Geology*, *217*(3–4), 305–321. https://doi.org/10.1016/j.margeo.2005.02.010

Bryan, S. E., & Ferrari, L. (2013). Large igneous provinces and silicic large igneous provinces: Progress in our understanding over the last 25 years. *Geological Society of America Bulletin*, *125*(7–8), 1053–1078. https://doi.org/10.1130/B30820.1

Buchs, D. M., Kerr, A. C., Brims, J. C., Zapata-Villada, J. P., Correa-Restrepo, T., & Rodríguez, G. (2018). Evidence for subaerial development of the Caribbean oceanic plateau in the Late Cretaceous and palaeo-environmental implications. *Earth and Planetary Science Letters*, *499*, 62–73. https://doi.org/10.1016/j.epsl.2018.07.020

Caron, M., Dall'Agnolo, S., Accarie, H., Barrera, E., Kauffman, E. G., Amédro, F., & Robaszynski, F. (2006). High-resolution stratigraphy of the Cenomanian–Turonian boundary interval at Pueblo (USA) and Wadi Bahloul (Tunisia): Stable isotope and bio-events correlation. *Geobios*, *39*(2), 171–200. https://doi.org/10.1016/j.geobios.2004.11.004

Clarkson, M. O., Stirling, C. H., Jenkyns, H. C., Dickson, A. J., Porcelli, D., Moy, C. M., et al. (2018). Uranium isotope evidence for two episodes of deoxygenation during Oceanic Anoxic Event 2. *Proceedings of the National Academy of Sciences*, *115*(12), 2918–2923. https://doi.org/10.1073/pnas.1715278115

Cohen, A. S., Coe, A. L., Bartlett, J. M., & Hawkesworth, C. J. (1999). Precise Re-Os ages of organic-rich mudrocks and the Os isotope composition of Jurassic seawater. *Earth and Planetary Science Letters*, *167*(3–4), 159–173. https://doi.org/10.1016/S0012-821X(99)00026-6

Courtillot, V., & Renne, P. R. (2003). On the ages of flood basalt events. *Comptes Rendus Geoscience*, *335*(1), 113–140. https://doi.org/10.1016/S1631-0713(03)00006-3

Cumming, V. M., Poulton, S. W., Rooney, A. D., & Selby, D. (2013). Anoxia in the terrestrial environment during the late Mesoproterozoic. *Geology*, *41*(5), 583–586. https://doi.org/10.1130/G34299.1

Desmares, D., Crognier, N., Bardin, J., Testé, M., Beaudoin, B., & Grosheny, D. (2016). A new proxy for Cretaceous paleoceanographic and paleoclimatic reconstructions: Coiling direction changes in the planktonic foraminifera Muricohedbergella delrioensis. *Palaeogeography, Palaeoclimatology, Palaeoecology*, *445*, 8–17. https://doi.org/10.1016/j.palaeo.2015.12.021

Dessert, C., Dupré, B., François, L. M., Schott, J., Gaillardet, J., Chakrapani, G., & Bajpai, S. (2001). Erosion of Deccan Traps determined by river geochemistry: Impact on the global climate and the $^{87}Sr/^{86}Sr$ ratio of seawater. *Earth and Planetary Science Letters*, *188*(3–4), 459–474. https://doi.org/10.1016/S0012-821X(01)00317-X

Dickson, A. J., Cohen, A. S., Coe, A. L., Davies, M., Shcherbinina, E. A., & Gavrilov, Y. O. (2015). Evidence for weathering and volcanism during the PETM from Arctic and Peri-Tethys osmium isotope records. *Palaeogeography, Palaeoclimatology, Palaeoecology*, *438*, 300–307. https://doi.org/10.1016/j.palaeo.2015.08.019

Dickson, A. J., Saker-Clark, M., Jenkyns, H. C., Bottini, C., Erba, E., Gorbanenko, O., et al. (2017). A Southern Hemisphere record of global trace-metal drawdown and orbital modulation of organic-matter burial across the Cenomanian–Turonian boundary (Ocean Drilling Program Site 1138, Kerguelen Plateau). *Sedimentology*, *64*(1), 186–203. https://doi.org/10.1111/sed.12303

Du Vivier, A. D., Jacobson, A. D., Lehn, G. O., Selby, D., Hurtgen, M. T., & Sageman, B. B. (2015). Ca isotope stratigraphy across the Cenomanian–Turonian OAE 2: Links between volcanism, seawater geochemistry, and the carbonate fractionation factor. *Earth and Planetary Science Letters*, *416*, 121–131. https://doi.org/10.1016/j.epsl.2015.02.001

Du Vivier, A. D. C., Selby, D., Takashima, R., & Nishi, H. (2015). Pacific $^{187}Os/^{188}Os$ isotope chemistry and U-Pb geochronology: Synchroneity of global Os isotope change across OAE 2. *Earth and Planetary Science Letters*, *428*, 204–216. https://doi.org/10.1016/j.epsl.2015.07.020

Du Vivier, A. D., Selby, D., Sageman, B. B., Jarvis, I., Gröcke, D. R., & Voigt, S. (2014). Marine $^{187}Os/^{188}Os$ isotope stratigraphy reveals the interaction of volcanism and ocean circulation during Oceanic Anoxic Event 2. *Earth and Planetary Science Letters*, *389*, 23–33. https://doi.org/10.1016/j.epsl.2013.12.024

Eldrett, J. S., Ma, C., Bergman, S. C., Lutz, B., Gregory, F. J., Dodsworth, P., et al. (2015). An astronomically calibrated stratigraphy of the Cenomanian, Turonian and earliest Coniacian from the Cretaceous Western Interior Seaway, USA: Implications for global chronostratigraphy. *Cretaceous Research*, *56*, 316–344. https://doi.org/10.1016/j.cretres.2015.04.010

Falzoni, F., Petrizzo, M. R., Jenkyns, H. C., Gale, A. S., & Tsikos, H. (2016). Planktonic foraminiferal biostratigraphy and assemblage composition across the Cenomanian–Turonian boundary interval at Clot Chevalier (Vocontian Basin, SE France). *Cretaceous Research*, *59*, 69–97. https://doi.org/10.1016/j.cretres.2015.10.028

Forster, A., Schouten, S., Moriya, K., Wilson, P. A., & Sinninghe Damsté, J. S. (2007). Tropical warming and intermittent cooling during the Cenomanian/Turonian oceanic anoxic event 2: Sea surface temperature records from the equatorial Atlantic. *Paleoceanography*, *22*, PA1219. https://doi.org/10.1029/2006PA001349

Friedrich, O., Erbacher, J., & Mutterlose, J. (2006). Paleoenvironmental changes across the Cenomanian/Turonian boundary event (Oceanic Anoxic Event 2) as indicated by benthic foraminifera from the Demerara Rise (ODP Leg 207). *Revue de Micropaleontologie*, *49*(3), 121–139. https://doi.org/10.1016/j.revmic.2006.04.003

Gale, A. S., & Christensen, W. K. (1996). Occurrence of the belemnite Actinocamax plenus in the Cenomanian of SE France and its significance. *Bulletin of the Geological Society of Denmark*, *43*, 68–77.

Gale, A. S., Jenkyns, H. C., Tsikos, H., van Breugel, Y., Sinninghe Damste, J. S., Bottini, C., et al. (2018). High-resolution bio-and chemostratigraphy of an expanded record of Oceanic Anoxic Event 2 (Late Cenomanian–Early Turonian) at Clot Chevalier, near Barrême, SE France (Vocontian Basin). *Newsletters on Stratigraphy*, *52*(1), 97–129. https://doi.org/10.1127/nos/2018/0445

Holmden, C., Jacobson, A. D., Sageman, B. B., & Hurtgen, M. T. (2016). Response of the Cr isotope proxy to Cretaceous Ocean Anoxic Event 2 in a pelagic carbonate succession from the Western Interior Seaway. *Geochimica et Cosmochimica Acta*, *186*, 277–295. https://doi.org/10.1016/j.gca.2016.04.039

Jarvis, I., Lignum, J. S., Gröcke, D. R., Jenkyns, H. C., & Pearce, M. A. (2011). Black shale deposition, atmospheric CO_2 drawdown, and cooling during the Cenomanian–Turonian Oceanic Anoxic Event. *Paleoceanography*, *26*, PA3201. https://doi.org/10.1029/2010PA002081

Jefferies, R. P. S. (1962). The palaeoecology of the *Actinocamax plenus* subzone (lowest Turonian) in the Anglo-Paris Basin. *Palaeontology*, *4*, 609–647.

Jefferies, R. P. S. (1963). The stratigraphy of the *Actinocamax plenus* Subzone (Turonian) in the Anglo-Paris Basin. *Proceedings of the Geologists Association*, *74*(1), 1–33. https://doi.org/10.1016/S0016-7878(63)80011-5

Jenkyns, H. C. (2010). Geochemistry of oceanic anoxic events. *Geochemistry, Geophysics, Geosystems*, *11*, Q03004. https://doi.org/10.1029/2009GC002788

Jenkyns, H. C., Dickson, A. J., Ruhl, M., & Boorn, S. H. (2017). Basalt-seawater interaction, the Plenus Cold Event, enhanced weathering and geochemical change: Deconstructing Oceanic Anoxic Event 2 (Cenomanian–Turonian, Late Cretaceous). *Sedimentology*, *64*(1), 16–43. https://doi.org/10.1111/sed.12305

Jones, C. E., & Jenkyns, H. C. (2001). Seawater strontium isotopes, oceanic anoxic events, and seafloor hydrothermal activity in the Jurassic and Cretaceous. *American Journal of Science*, *301*(2), 112–149. https://doi.org/10.2475/ajs.301.2.112

Jones, M. M., Sageman, B. B., Oakes, R. L., Parker, A. L., Leckie, R. M., Bralower, T. J., et al. (2019). Astronomical pacing of relative sea level during Oceanic Anoxic Event 2: Preliminary studies of the expanded SH#1 Core, Utah, USA. *Geological Society of America Bulletin*, *131*(9–10), 1702–1722. https://doi.org/10.1130/B32057.1

Jones, M. M., Sageman, B. B., Selby, D., Jicha, B. R., Singer, B. S., & Titus, A. L. (2020). Regional chronostratigraphic synthesis of the Cenomanian–Turonian oceanic anoxic event 2 (OAE 2) interval, Western Interior Basin (USA): New Re-Os chemostratigraphy and $^{40}Ar/^{39}Ar$ geochronology. *Geological Society of America Bulletin*. https://doi.org/10.1130/B35594.1

Kerr, A. C. (2014). Oceanic Plateaus. In H. D. Holland & K. K. Turekian (Eds.), *Treatise on geochemistry: Vol: 4: The crust* (pp. 631–667). Amsterdam: Elsevier. https://doi.org/10.1016/B978-0-08-095975-7.00320-X

Kingsbury, C. G., Kamo, S. L., Ernst, R. E., Söderlund, U., & Cousens, B. L. (2018). U-Pb geochronology of the plumbing system associated with the Late Cretaceous Strand Fiord Formation, Axel Heiberg Island, Canada: Part of the 130-90 Ma High Arctic large igneous province. *Journal of Geodynamics*, *118*, 106–117. https://doi.org/10.1016/j.jog.2017.11.001

Kuhnt, W., Thurow, J., Wiedmann, J., & Herbin, J. P. (1986). Oceanic anoxic conditions around the Cenomanian/Turonian boundary and the response of the biota. In P. A. Meyers, S. C. Brassell, E. T. Degenns (Eds.), *Biogeochemistry of black shales* (Vol. 60, pp. 205–246). Hamburg: Mitteilungen der Geologisch–Palaöntologisches Institut der Universität.

Kump, L. R., Brantley, S. L., & Arthur, M. A. (2000). Chemical weathering, atmospheric CO_2, and climate. *Annual Review of Earth and Planetary Sciences*, *28*(1), 611–667. https://doi.org/10.1146/annurev.earth.28.1.611

Kuroda, J., Ogawa, N. O., Tanimizu, M., Coffin, M. F., Tokuyama, H., Kitazato, H., & Ohkouchi, N. (2007). Contemporaneous massive subaerial volcanism and Late Cretaceous Oceanic Anoxic Event 2. *Earth and Planetary Science Letters*, *256*(1–2), 211–223. https://doi.org/10.1016/j.epsl.2007.01.027

Kuypers, M. M., Pancost, R. D., & Damste, J. S. S. (1999). A large and abrupt fall in atmospheric CO_2 concentration during Cretaceous times. *Nature*, *399*(6734), 342–345. https://doi.org/10.1038/20659

Leckie, R. M., Yuretich, R. F., West, O. L., Finkelstein, D., & Schmidt, M. (1998). Paleoceanography of the southwestern Western Interior Sea during the time of the Cenomanian-Turonian boundary (Late Cretaceous). In W. E. Dean & M. A. Arthur (Eds.), *Stratigraphy and paleoenvironments of the Cretaceous Western Interior Seaway* (Vol. 6, pp. 101–126). USA: SEPM Concepts in Sedimentology and Paleontology.

Ma, C., Meyers, S. R., Sageman, B. B., Singer, B. S., & Jicha, B. R. (2014). Testing the astronomical time scale for oceanic anoxic event 2, and its extension into Cenomanian strata of the Western Interior Basin (USA). *Geological Society of America Bulletin*, *126*(7–8), 974–989. https://doi.org/10.1130/B30922.1

Meisel, T., Walker, R. J., Irving, A. J., & Lorand, J. P. (2001). Osmium isotopic compositions of mantle xenoliths: A global perspective. *Geochimica et Cosmochimica Acta*, *65*(8), 1311–1323. https://doi.org/10.1016/S0016-7037(00)00566-4

Meyers, S. R., Siewert, S. E., Singer, B. S., Sageman, B. B., Condon, D. J., Obradovich, J. D., et al. (2012). Intercalibration of radioisotopic and astrochronologic time scales for the Cenomanian-Turonian boundary interval, Western Interior Basin, USA. *Geology*, *40*(1), 7–10. https://doi.org/10.1130/G32261.1

Miller, K. G., Sugarman, P. J., Browning, J. V., Olsson, R. K., Pekar, S. F., Reilly, T. J., et al. (1998). Bass River Site. In K. G. Miller, P. J. Sugarman, J. V. Browning, et al. (Eds.), *Proceedings of the Ocean Drilling Program*, *Initial Reports* (Vol. 174AX, pp. 5–43). College Station, TX: Ocean Drilling Program. https://doi.org/10.2973/odp.proc.ir.174ax.101.1998

Neal, C. R., Mahoney, J. J., Kroenke, L. W., Duncan, R. A., & Petterson, M. G. (1997). The Ontong–Java Plateau. In J. J. Mahoney & M. F. Coffin (Eds.), *Large igneous provinces: Continental, oceanic and planetary flood volcanism* (pp. 183–216). Washington, DC: American Geophysical Union. https://doi.org/10.1029/GM100p0183

Nederbragt, A. J., & Fiorentino, A. (1999). Stratigraphy and palaeoceanography of the Cenomanian-Turonian Boundary Event in Oued Mellegue, north-western Tunisia. *Cretaceous Research*, *20*(1), 47–62. https://doi.org/10.1006/cres.1998.0136

Nowell, G. M., Luguet, A., Pearson, D. G., & Horstwood, M. S. A. (2008). Precise and accurate $^{186}Os/^{188}Os$ and $^{187}Os/^{188}Os$ measurements by multi-collector plasma ionisation mass spectrometry (MC-ICP-MS) part I: Solution analyses. *Chemical Geology*, *248*(3–4), 363–393. https://doi.org/10.1016/j.chemgeo.2007.10.020

O'Brien, C. L., Robinson, S. A., Pancost, R. D., Damsté, J. S. S., Schouten, S., Lunt, D. J., et al. (2017). Cretaceous sea-surface temperature evolution: Constraints from TEX_{86} and planktonic foraminiferal oxygen isotopes. *Earth-Science Reviews*, *172*, 224–247. https://doi.org/10.1016/j.earscirev.2017.07.012

O'Connor, L. K., Jenkyns, H. C., Robinson, S. A., Remmelzwaal, S. R., Batenburg, S. J., Parkinson, I. J., & Gale, A. S. (2020). A re-evaluation of the Plenus Cold Event, and the links between CO_2, temperature, and seawater chemistry during OAE 2. *Paleoceanography and Paleoclimatology*, *35*, e2019PA003631. https://doi.org/10.1029/2019PA003631

Ostrander, C. M., Owens, J. D., & Nielsen, S. G. (2017). Constraining the rate of oceanic deoxygenation leading up to a Cretaceous Oceanic Anoxic Event (OAE-2: ~94 Ma). *Science Advances*, *3*, e1701020. https://doi.org/10.1126/sciadv.1701020

Owens, J. D., Lyons, T. W., & Lowery, C. M. (2018). Quantifying the missing sink for global organic carbon burial during a Cretaceous oceanic anoxic event. *Earth and Planetary Science Letters*, *499*, 83–94. https://doi.org/10.1016/j.epsl.2018.07.021

Paquay, F. S., & Ravizza, G. (2012). Heterogeneous seawater $^{187}Os/^{188}Os$ during the Late Pleistocene glaciations. *Earth and Planetary Science Letters*, *349–350*, 126–138. https://doi.org/10.1016/j.epsl.2012.06.051

Paul, C. R. C., Lamolda, M. A., Mitchell, S. F., Vaziri, M. R., Gorostidi, A., & Marshall, J. D. (1999). The Cenomanian-Turonian boundary at Eastbourne (Sussex, UK): A proposed European reference section. *Palaeogeography, Palaeoclimatology, Palaeoecology*, *150*(1–2), 83–121. https://doi.org/10.1016/S0031-0182(99)00009-7

Percival, L. M. E., Jenkyns, H. C., Mather, T. A., Dickson, A. J., Batenburg, S. J., Ruhl, M., et al. (2018). Does large igneous province volcanism always perturb the mercury cycle? Comparing the records of Oceanic Anoxic Event 2 and the end-Cretaceous to other Mesozoic events. *American Journal of Science*, *318*(8), 799–860. https://doi.org/10.2475/08.2018.01

Peucker-Ehrenbrink, B., & Jahn, B. M. (2001). Rhenium-osmium isotope systematics and platinum group element concentrations: Loess and the upper continental crust. *Geochemistry, Geophysics, Geosystems*, *2*, 1061. https://doi.org/10.1029/2001GC000172

Peucker-Ehrenbrink, B., & Ravizza, G. (2000). The marine osmium isotope record. *Terra Nova*, *12*(5), 205–219. https://doi.org/10.1046/j.1365-3121.2000.00295.x

Pogge von Strandmann, P. A. E., Jenkyns, H. C., & Woodfine, R. G. (2013). Lithium isotope evidence for enhanced weathering during Oceanic Anoxic Event 2. *Nature Geoscience*, *6*(8), 668–672. https://doi.org/10.1038/ngeo1875

Robinson, S. A., Dickson, A. J., Pain, A., Jenkyns, H. C., O'Brien, C. L., Farnsworth, A., & Lunt, D. J. (2019). Southern Hemisphere sea-surface temperatures during the Cenomanian–Turonian: Implications for the termination of Oceanic Anoxic Event 2. *Geology*, *47*(2), 131–134. https://doi.org/10.1130/G45842.1

Robinson, S. A., Heimhofer, U., Hesselbo, S. P., & Petrizzo, M. R. (2017). Mesozoic climates and oceans—A tribute to Hugh Jenkyns and Helmut Weissert. *Sedimentology*, *64*(1), 1–15. https://doi.org/10.1111/sed.12349

Rooney, A. D., Selby, D., Lloyd, J. M., Roberts, D. H., Lückge, A., Sageman, B. B., & Prouty, N. G. (2016). Tracking millennial-scale Holocene glacial advance and retreat using osmium isotopes: Insights from the Greenland ice sheet. *Quaternary Science Reviews*, *138*, 49–61. https://doi.org/10.1016/j.quascirev.2016.02.021

Sageman, B. B., Meyers, S. R., & Arthur, M. A. (2006). Orbital time scale and new C-isotope record for Cenomanian-Turonian boundary stratotype. *Geology*, *34*(2), 125–128. https://doi.org/10.1130/G22074.1

Scaife, J. D., Ruhl, M., Dickson, A. J., Mather, T. A., Jenkyns, H. C., Percival, L. M. E., et al. (2017). Sedimentary mercury enrichments as a marker for submarine large igneous province volcanism? Evidence from the Mid-Cenomanian event and Oceanic Anoxic Event 2 (Late Cretaceous). *Geochemistry, Geophysics, Geosystems*, *18*, 4253–4275. https://doi.org/10.1002/2017GC007153

Schaller, M. F., Wright, J. D., Kent, D. V., & Olsen, P. E. (2012). Rapid emplacement of the Central Atlantic Magmatic Province as a net sink for CO_2. *Earth and Planetary Science Letters*, *323–324*, 27–39. https://doi.org/10.1016/j.epsl.2011.12.028

Schlanger, S. O., & Jenkyns, H. C. (1976). Cretaceous oceanic anoxic events: Causes and consequences. *Geologie en Mijnbouw*, *55*, 179–184.

Schröder-Adams, C. J., Herrle, J. O., Selby, D., Quesnel, A., & Froude, G. (2019). Influence of the High Arctic Igneous Province on the Cenomanian/Turonian boundary interval, Sverdrup Basin, High Canadian Arctic. *Earth and Planetary Science Letters*, *511*, 76–88. https://doi.org/10.1016/j.epsl.2019.01.023

Selby, D., & Creaser, R. A. (2003). Re–Os geochronology of organic rich sediments: An evaluation of organic matter analysis methods. *Chemical Geology*, *200*(3–4), 225–240. https://doi.org/10.1016/S0009-2541(03)00199-2

Sinninghe Damsté, J. S., van Bentum, E. C., Reichart, G. J., Pross, J., & Schouten, S. (2010). A CO_2 decrease-driven cooling and increased latitudinal temperature gradient during the mid-Cretaceous Oceanic Anoxic Event 2. *Earth and Planetary Science Letters*, *293*(1–2), 97–103. https://doi.org/10.1016/j.epsl.2010.02.027

Snow, L. J., Duncan, R. A., & Bralower, T. J. (2005). Trace element abundances in the Rock Canyon Anticline, Pueblo, Colorado, marine sedimentary section and their relationship to Caribbean plateau construction and oxygen anoxic event 2. *Paleoceanography*, *20*, PA3005. https://doi.org/10.1029/2004PA001093

Storey, M., Mahoney, J. J., Saunders, A. D., Duncan, R. A., Kelley, S. P., & Coffin, M. F. (1995). Timing of hot spot-related volcanism and the breakup of Madagascar and India. *Science*, *267*(5199), 852–855. https://doi.org/10.1126/science.267.5199.852

Sugarman, P. J., Miller, K. G., Olsson, R. K., Browning, J. V., Wright, J. D., De Romero, L. M., et al. (1999). The Cenomanian/Turonian carbon burial event, Bass River, NJ, USA; geochemical, paleoecological, and sea-level changes. *The Journal of Foraminiferal Research*, *29*, 438–452.

Sullivan, D. L., Brandon, A. D., Eldrett, J., Bergman, S. C., Minisini, D., & Wright, S. (2020). High resolution osmium data record three distinct pulses of magmatic activity during Cretaceous Oceanic Anoxic Event 2 (OAE-2). *Geochimica et Cosmochimica Acta*, *285*, 257–273. https://doi.org/10.1016/j.gca.2020.04.002

Sweere, T. C., Dickson, A. J., Jenkyns, H. C., Porcelli, D., Elrick, M., van den Boorn, S. H., & Henderson, G. M. (2018). Isotopic evidence for changes in the zinc cycle during Oceanic Anoxic Event 2 (Late Cretaceous). *Geology*, *46*(5), 463–466. https://doi.org/10.1130/G40226.1

Tegner, C., Storey, M., Holm, P. M., Thorarinsson, S. B., Zhao, X., Lo, C. H., & Knudsen, M. F. (2011). Magmatism and Eurekan deformation in the High Arctic Large Igneous Province: ^{40}Ar-^{39}Ar age of Kap Washington Group volcanics. North Greenland. *Earth and Planetary Science Letters*, *303*(3–4), 203–214. https://doi.org/10.1016/j.epsl.2010.12.047

Tsikos, H., Jenkyns, H. C., Walsworth-Bell, B., Petrizzo, M. R., Forster, A., Kolonic, S., et al. (2004). Carbon-isotope stratigraphy recorded by the Cenomanian–Turonian Oceanic Anoxic Event: correlation and implications based on three key localities. *Journal of the Geological Society of London*, *161*(4), 711–719. https://doi.org/10.1144/0016-764903-077

Turgeon, S. C., & Creaser, R. A. (2008). Cretaceous oceanic anoxic event 2 triggered by a massive magmatic episode. *Nature*, *454*(7202), 323–326. https://doi.org/10.1038/nature07076

van Bentum, E. C., Hetzel, A., Brumsack, H. J., Forster, A., Reichart, G. J., & Damste, J. S. S. (2009). Reconstruction of water column anoxia in the equatorial Atlantic during the Cenomanian–Turonian oceanic anoxic event using biomarker and trace metal proxies. *Palaeogeography, Palaeoclimatology, Palaeoecology*, *280*(3–4), 489–498. https://doi.org/10.1016/j.palaeo.2009.07.003

van Bentum, E. C., Reichart, G. J., & Damsté, J. S. S. (2012). Organic matter provenance, palaeoproductivity and bottom water anoxia during the Cenomanian/Turonian oceanic anoxic event in the Newfoundland Basin (northern proto North Atlantic Ocean). *Organic Geochemistry*, *50*, 11–18. https://doi.org/10.1016/j.orggeochem.2012.05.013

van Helmond, N. A., Sluijs, A., Papadomanolaki, N., Plint, A. G., Gröcke, D., Pearce, M., et al. (2016). Equatorward phytoplankton migration during a cold spell within the Late Cretaceous super-greenhouse. *Biogeosciences*, *13*(9), 2859–2872. https://doi.org/10.5194/bg-13-2859-2016

van Helmond, N. A. G. M., Sluijs, A., Reichart, G. J., Sinninghe Damsté, J. S., Slomp, C. P., & Brinkhuis, H. (2014). A perturbed hydrological cycle during Oceanic Anoxic Event 2. *Geology*, *42*(2), 123–126. https://doi.org/10.1130/G34929.1

van Helmond, N. A. G. M., Sluijs, A., Sinninghe Damsté, J. S., Reichart, G. J., Voigt, S., Erbacher, J., et al. (2015). Freshwater discharge controlled deposition of Cenomanian–Turonian black shales on the NW European epicontinental shelf (Wunstorf, northern Germany). *Climate of the Past*, *11*(3), 495–508. https://doi.org/10.5194/cp-11-495-2015

Voigt, S., Erbacher, J., Mutterlose, J., Weiss, W., Westerhold, T., Wiese, F., et al. (2008). The Cenomanian Turonian of the Wunstorf section (North Germany): Global stratigraphic reference section and new orbital time scale for Oceanic Anoxic Event 2. *Newsletters on Stratigraphy*, *43*(1), 65–89. https://doi.org/10.1127/0078-0421/2008/0043-0065

Voigt, S., Gale, A. S., & Voigt, T. (2006). Sea-level change, carbon cycling and palaeoclimate during the Late Cenomanian of northwest Europe; an integrated palaeoenvironmental analysis. *Cretaceous Research*, *27*(6), 836–858. https://doi.org/10.1016/j.cretres.2006.04.005

Zheng, X.-Y., Jenkyns, H. C., Gale, A. S., Ward, D. J., & Henderson, G. M. (2013). Changing ocean circulation and hydrothermal inputs during Ocean Anoxic Event 2 (Cenomanian-Turonian): Evidence from Nd-isotopes in the European shelf sea. *Earth and Planetary Science Letters*, *375*, 338–348. https://doi.org/10.1016/j.epsl.2013.05.053